Author(s): Qu, Zengcai & Tuovinen, Toni & Hinkkanen, Marko

Title: Minimizing losses of a synchronous reluctance motor drive taking into account core losses and magnetic saturation

Year: 2014

Version: Post print

Please cite the original version:

Qu, Zengcai & Tuovinen, Toni & Hinkkanen, Marko. 2014. Minimizing losses of a synchronous reluctance motor drive taking into account core losses and magnetic saturation. 2014 16th European Conference on Power Electronics and Applications (EPE'14-ECCE Europe). 10. DOI: 10.1109/epe.2014.6910929.

Minimizing Losses of a Synchronous Reluctance Motor Drive Taking into Account Core Losses and Magnetic Saturation

Zengcai Qu, Toni Tuovinen and Marko Hinkkanen
Aalto University School of Electrical Engineering
Department of Electrical Engineering and Automation
P.O. BOX 13000, FI-00076 Aalto, Espoo, Finland
E-mails: zengcai.qu@aalto.fi, toni.tuovinen@aalto.fi, marko.hinkkanen@aalto.fi

Keywords

<<Efficiency>>, <<Electrical drive>>, <<Synchronous motor>>, <<Sensorless control>>, << Vector control>>.

Abstract

This paper proposes a loss-minimizing controller for synchronous reluctance motor drives. The proposed method takes core losses and magnetic saturation effects into account. The core-loss model consists of hysteresis losses and eddy-current losses. Magnetic saturation is modeled using two-dimensional power functions considering cross coupling between the d- and q-axes. The efficiency optimal d-axis current is calculated offline using the loss model and motor parameters. Instead of generating a look-up table, an approximate function was fitted to the loss-minimizing results. The loss-minimizing method is applied in a motion-sensorless drive and the results are validated by measurements.

Introduction

In vector control of a synchronous reluctance motor (SyRM), certain speed and torque can be achieved by different combinations of d- and q-axes currents. The total losses can be minimized by adjusting the d- and q-axes current ratio. Generally, there are two categories of loss-minimizing controllers: the loss-model based controller (LMC) which uses the motor model and parameters to calculate the loss-minimizing currents, and the online search controller (SC) which adjusts the current vector online based on the feedback of input power measurement. Since the SC does not require any motor parameters beforehand, the bulk of the work to determine the motor parameters can be avoided. However, the searching process may cause unwanted losses and torque ripples. Furthermore, it might be sensitive to the measurement noise and errors. The main disadvantage of the LMC is its dependancy on the motor parameters. However, the motor parameters are required in many parts of electric drives, e.g., they are required in speed sensorless control. Therefore, the LMC can be a better option in the case of known motor parameters.

The total losses in the SyRM can be formulated as a loss function of control variables and the motor parameters. By minimizing this function, the efficiency optimal control variable, e.g., the d-axis current, can be found. Simple LMCs assuming constant inductances and constant core-loss resistance can be found in the literature [1, 2]. However, the inductances vary with the stator currents and the core-loss resistance is a function of the flux and speed. Magnetic saturation effects were ignored for simplification in [3–11], and only a few LMCs have taken magnetic saturation into account [12,13]. However, parameter sensitivity of loss minimization was studied in [14] and it shows that the inductance variations due to magnetic saturation affect the optimal current significantly. The core losses can be modeled using a constant resistance if the hysteresis losses are omitted. In [4], the core losses were modeled as hysteresis losses and eddy-current losses. The stray-load losses were also taken into account in [9] and [10]. The nonlinear magnetic saturation model and core-loss model usually result in a complicated loss function.

An analytical solution of loss minimization is difficult to derive. However, iteration methods can be used. For example, the cross-magnetic saturation was modeled and the optimum current was derived using an iteration method in [13]. Simple core-loss and magnetic saturation models were applied in [8], but the core-loss resistance and the inductances were estimated by the extended Kalman filter.

Neural networks (NNs) and fuzzy logic have been used in the LMCs. In [15], a NN was used as an adaptive model of the SyRM. The NN was trained online, and the input is the torque reference and the outputs are the d-q axes current references. In [7], the loss function with constant inductances and core-loss resistance was applied, and an offline-trained NN was used to map the optimal current. These methods are actually similar to the simple LMCs since they just map the loss function to neural networks.

This paper aims to break the tradeoff between accuracy and complexity of LMCs. Nonlinear core-loss and magnetic saturation models make the loss function too complicated to get an analytical solution. Iterative methods can be used to find the minimum points of the loss function. However, it is computation demanding for online utilization. A general idea of the proposed LMC is to calculate the optimal currents iteratively offline and then fit the results to a simple function for online use. A similar approach can be found in [16], where the core-loss and magnetic saturation parameters were obtained from finite element analysis. The optimal currents were calculated offline. A loss-minimizing look-up table was generated from the off-line calculation results. However, the loss minimization was not validated by experimental measurement.

In this paper, both the core losses and magnetic saturation are taken into account. The core-loss model consists of hysteresis losses and eddy current losses, and the magnetic saturation is modeled using two-dimensional power functions taking into account cross coupling between the d- and q-axes. The parameters of core losses and magnetic saturation are determined by experimental measurements. An iteration method is used to calculate the optimal d-axis current offline for given operating points. The results are fitted to a simple function which can be easily implemented online. Hence, extensive computation can be avoided in real-time control. The proposed method is validated by experiments of a 6.7-kW SyRM.

SyRM Model

Space-vector Model

Fig. 1 shows the dynamic space-vector model of an SyRM. The d-axis of the rotating coordinate system is defined as the direction of the maximum inductance. Real space vectors will be used in the model. For example, the stator-current vector is $\boldsymbol{i}_\mathrm{s} = [i_\mathrm{d}, i_\mathrm{q}]^\mathrm{T}$, where i_d and i_q are the components of the vector and the matrix transpose is marked with the superscript T. The magnitude is denoted by $i_\mathrm{s} = \sqrt{i_\mathrm{d}^2 + i_\mathrm{q}^2}$. The orthogonal rotation matrix is $\mathbf{J} = \left[\begin{smallmatrix} 0 & -1 \\ 1 & 0 \end{smallmatrix}\right]$. Per-unit quantities will be used.

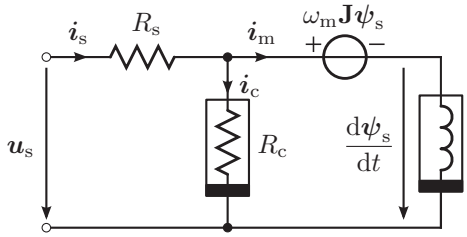

Figure 1: Dynamic space-vector model of a SyRM in rotor coordinates.

The voltage equation is

$$\frac{\mathrm{d}\boldsymbol{\psi}_\mathrm{s}}{\mathrm{d}t} = \boldsymbol{u}_\mathrm{s} - R_\mathrm{s}\boldsymbol{i}_\mathrm{s} - \omega_\mathrm{m}\mathbf{J}\boldsymbol{\psi}_\mathrm{s} \tag{1}$$

where $\boldsymbol{\psi}_\mathrm{s}$ is the stator-flux vector, $\boldsymbol{u}_\mathrm{s}$ the stator-voltage vector, R_s the stator resistance, $\boldsymbol{i}_\mathrm{s}$ the stator current, and ω_m is the angular speed of the rotor. The core-loss current is $\boldsymbol{i}_\mathrm{c} = \boldsymbol{i}_\mathrm{s} - \boldsymbol{i}_\mathrm{m}$, where $\boldsymbol{i}_\mathrm{m}$ is the magnetizing currrent which is a nonlinear function of the flux due to magnetic saturation. The core losses are modeled as a nonlinear resistance R_c. The electromagnetic torque is given by

$$T_\mathrm{e} = i_\mathrm{mq}\psi_\mathrm{d} - i_\mathrm{md}\psi_\mathrm{q} \tag{2}$$

Magnetic Saturation

The effects of magnetic saturation are often an important issue in model-based loss minimization. The stator inductances vary with the fluxes (or the currents) of both axes. The inductances can be obtained from finite-element methods or measurements. The look-up table is usually computationally inefficient and needs interpolation. As reviewed in [17], the measured data are often fitted to explicit functions. The magnetic saturation effects can be modeled as current functions of the fluxes [17] using two-dimensional power functions:

$$i_{\mathrm{md}}(\psi_{\mathrm{d}},\psi_{\mathrm{q}}) = \frac{\psi_{\mathrm{d}}}{L_{\mathrm{du}}}\left[1 + (\alpha|\psi_{\mathrm{d}}|)^a + \frac{\gamma L_{\mathrm{du}}}{d+2}|\psi_{\mathrm{d}}|^c|\psi_{\mathrm{q}}|^{d+2}\right] \tag{3a}$$

$$i_{\mathrm{mq}}(\psi_{\mathrm{d}},\psi_{\mathrm{q}}) = \frac{\psi_{\mathrm{q}}}{L_{\mathrm{qu}}}\left[1 + (\beta|\psi_{\mathrm{q}}|)^b + \frac{\gamma L_{\mathrm{qu}}}{c+2}|\psi_{\mathrm{d}}|^{c+2}|\psi_{\mathrm{q}}|^{d}\right] \tag{3b}$$

where L_{du} and L_{qu} are the unsaturated inductances, and α, β, γ, a, b, c, and d are nonnegative constants. The fitted parameters of the 6.7-kW SyRM are shown in Table I and the fitting results are shown in Fig. 2.

Table I: Fitted per-unit parameters [17].

L_{du}	L_{qu}	α	β	γ	a	b	c	d
2.73	0.843	0.847	3.84	2.37	6.61	1.33	0.41	0

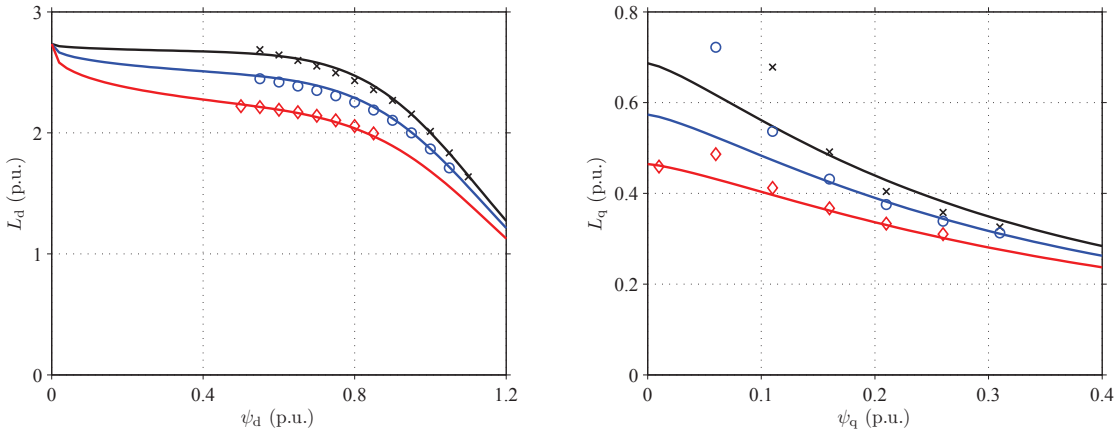

(a) (b)

Figure 2: Results of curve fitting to experimental data [17]: (a) L_{d} as a function of ψ_{d} for three different values of ψ_{q}; (b) L_{q} as a function of ψ_{q} for three different values of ψ_{d}. In (a), the values of ψ_{q} are 0.1 p.u. (black line), 0.2 p.u. (blue line) and 0.3 p.u. (red line). In (b), the values of ψ_{d} are 0.6 p.u. (black line), 0.8 p.u. (blue line) and 1.0 p.u. (red line).

Core Losses

The core losses can be divided into two parts: hysteresis losses and classical eddy-current losses. In steady state, the stator core losses are classically modeled as a function of the rotor frequency ω_{m} and the stator-flux magnitude ψ_{s},

$$P_{\mathrm{Fe}} = \Lambda_{\mathrm{Hy}}|\omega_{\mathrm{m}}|\,\psi_{\mathrm{s}}^2 + G_{\mathrm{Ft}}\omega_{\mathrm{m}}^2\psi_{\mathrm{s}}^2 \tag{4}$$

where the first term corresponds to the hysteresis losses and the second term corresponds to the eddy-current losses [18]. The hysteresis losses are proportional to the frequency, while the eddy-current losses are proportional to the square of the frequency. The constants Λ_{Hy} and G_{Ft} determine the ratio between the loss components at a given stator flux and angular frequency. The core losses are typically modeled using a core-loss resistor R_{c} in steady state. The core-loss resistance corresponding to (4) becomes

$$R_{\mathrm{c}} = \frac{1}{\Lambda_{\mathrm{Hy}}/|\omega_{\mathrm{m}}| + G_{\mathrm{Ft}}} \tag{5}$$

It can be seen that the core-loss resistance R_c is constant if the hysteresis losses are omitted ($\Lambda_\mathrm{Hy} = 0$). The parameters can be identified using series of no-load tests at different frequencies. The fitted parameters for the 6.7-kW SyRM are $\Lambda_\mathrm{Hy} = 0.018$ p.u. and $G_\mathrm{Ft} = 0.042$ p.u. Fig. 3 shows the core-loss curves and the measured core losses at different flux levels.

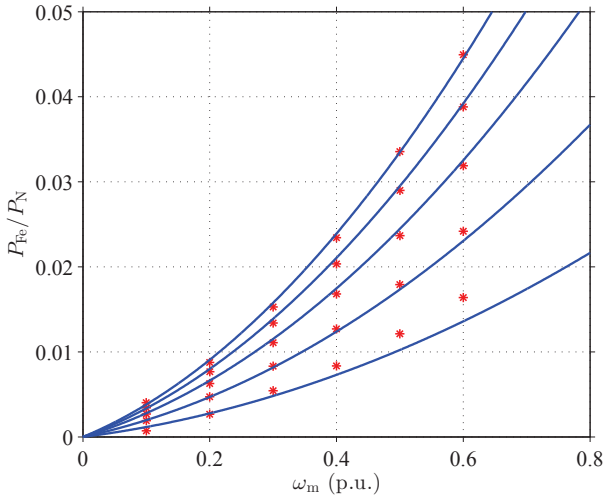

Figure 3: Core-loss curves as a function of angular frequency ω_m for $\Lambda_\mathrm{Hy} = 0.018$ p.u. and $G_\mathrm{Ft} = 0.042$ p.u. Markers show the measured core losses from no-load tests (different flux levels were applied at each stator frequency).

Loss Minimization

Conventional LMC

Many LMCs are based on constant motor parameters R_c, L_d, and L_q. The per-unit losses are given by

$$P_\mathrm{loss} = \left[R_\mathrm{s} + (R_\mathrm{s} + R_\mathrm{c})\,\frac{\omega_\mathrm{m}^2 L_\mathrm{d}^2}{R_\mathrm{c}^2}\right] i_\mathrm{md}^2 + \left[R_\mathrm{s} + (R_\mathrm{s} + R_\mathrm{c})\,\frac{\omega_\mathrm{m}^2 L_\mathrm{q}^2}{R_\mathrm{c}^2}\right] i_\mathrm{mq}^2 + \left[\frac{2R_\mathrm{s}}{R_\mathrm{c}}\omega_\mathrm{m}(L_\mathrm{d} - L_\mathrm{q})\right] i_\mathrm{md} i_\mathrm{mq} \tag{6}$$

Let the ratio of d- and q-axis currents be $\zeta = i_\mathrm{mq}/i_\mathrm{md}$. By solving $\partial P_\mathrm{loss}/\partial\zeta = 0$, the optimal current ratio is given by

$$\zeta_\mathrm{opt} = \frac{i_\mathrm{mq,opt}}{i_\mathrm{md,opt}} = \sqrt{\frac{R_\mathrm{s}R_\mathrm{c}^2 + (R_\mathrm{s} + R_\mathrm{c})\omega_\mathrm{m}^2 L_\mathrm{d}^2}{R_\mathrm{s}R_\mathrm{c}^2 + (R_\mathrm{s} + R_\mathrm{c})\omega_\mathrm{m}^2 L_\mathrm{q}^2}} \tag{7}$$

The current $\boldsymbol{i}_\mathrm{m}$ cannot be measured and controlled directly. The optimal d-axis stator current which compensates the core-loss current component is given by

$$i_\mathrm{sd,opt} = i_\mathrm{md,opt} - \omega_\mathrm{m} L_\mathrm{q} i_\mathrm{mq,opt}/R_\mathrm{c} \tag{8}$$

where

$$i_\mathrm{md,opt} = \sqrt{\frac{|T_\mathrm{e}|}{(L_\mathrm{d} - L_\mathrm{q})\zeta_\mathrm{opt}}}, \quad i_\mathrm{mq,opt} = \mathrm{sign}(T_\mathrm{e})\zeta_\mathrm{opt} i_\mathrm{md,opt} \tag{9}$$

The result leads to a simple LMC solution. However, the variations of the motor parameters may cause errors in the loss minimization. The stator resistance varies with temperature, the core-loss model is a nonlinear function of the flux and rotor frequency, and L_d and L_q change with the stator fluxes due to magnetic saturation.

Proposed LMC

Offline Calculation of Loss Minimization

Substituting the magnetic saturation model (3) into the torque equation (2),

$$T_{\mathrm{e}} = \frac{\psi_{\mathrm{d}}\psi_{\mathrm{q}}}{L_{\mathrm{qu}}}\left[1 + (\beta|\psi_{\mathrm{q}}|)^b + \frac{\gamma L_{\mathrm{qu}}}{c{+}2}|\psi_{\mathrm{d}}|^{c+2}|\psi_{\mathrm{q}}|^d\right] - \frac{\psi_{\mathrm{d}}\psi_{\mathrm{q}}}{L_{\mathrm{du}}}\left[1 + (\alpha|\psi_{\mathrm{d}}|)^a + \frac{\gamma L_{\mathrm{du}}}{d{+}2}|\psi_{\mathrm{d}}|^c|\psi_{\mathrm{q}}|^{d+2}\right] \quad (10)$$

If the torque T_{e} and the d-axis flux ψ_{d} are given, the q-axis flux ψ_{q} is the only unknown variable in (10). The analytical solution of ψ_{q} is difficult to be derived since (10) is a complicated power equation. The equation is solved numerically. Then, using ψ_{d} and ψ_{q}, the magnetizing current components i_{md} and i_{mq} can be calculated based on the saturation model (2).

If the speed ω_{m} is given, the core-loss current can be calculated as

$$\boldsymbol{i}_{\mathrm{c}} = \frac{\omega_{\mathrm{m}}\mathbf{J}\boldsymbol{\psi}_{\mathrm{s}}}{R_{\mathrm{c}}} \quad (11)$$

Summing the magnetizing current and the core-loss current, the stator current is

$$\boldsymbol{i}_{\mathrm{s}} = \boldsymbol{i}_{\mathrm{m}} + \boldsymbol{i}_{\mathrm{c}} \quad (12)$$

Finally, the total power losses can be calculated as

$$P_{\mathrm{loss}} = R_{\mathrm{s}}i_{\mathrm{s}}^2 + R_{\mathrm{c}}i_{\mathrm{c}}^2 \quad (13)$$

where the first term corresponds to the copper losses and the second term corresponds to the core losses. The calculation flow chart of the power losses for a given T_{e}, ω_{m} and ψ_{d} are shown in Fig. 4.

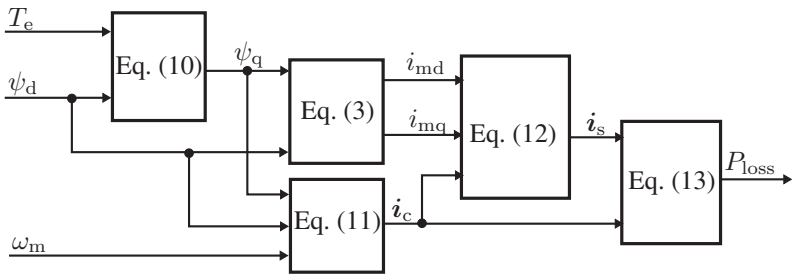

Figure 4: Calculation of the power losses for given torque, speed and d-axis flux.

The loss curves as functions of i_{sd} for different torque and speed are shown in Fig. 5. It can be seen that the total losses highly depend on the torque and vary slightly with the speed.

In order to find the minimum losses, ψ_{d} is changed iteratively and the minimum P_{loss} is searched numerically. When the minimum P_{loss} is found, the corresponding d-axis i_{sd} is saved as the loss-minimizing current for given T_{e} and ω_{m}. Iterative methods are used in solving (10) and in searching the minimum losses. Hence, it is computationally demanding to calculate the loss-minimizing current online for real-time control. The calculations of the proposed method are made offline and the results are saved for online use.

Fig. 6 shows the calculated optimal d-axis currents as function of torque for speeds of 0.2, 0.4 and 0.6 p.u. As can be seen, the optimal i_{sd} increases with the increase of torque. The speed slightly affects the optimal current, higher speed leads to lower loss-minimizing i_{sd}.

Instead of generating a look-up table for online implementation, the calculated optimal current can be fitted to a simple function:

$$i_{\mathrm{sd,opt}} = (A + B|\omega_{\mathrm{m}}|)|T_{\mathrm{e}}|^{(C+D|\omega_{\mathrm{m}}|)} \quad (14)$$

where A, B, C, and D are fitting parameters. The fitted per-unit parameters are: $A = 0.5561, B = 0.1395, C = 0.5223$ and $D = 0.213$. The fitting result is shown in Fig. 6. The benefits of using this approximate function are: simple implementation; no need for online iterative computation; loss measurements can be used to adjust the fitting result.

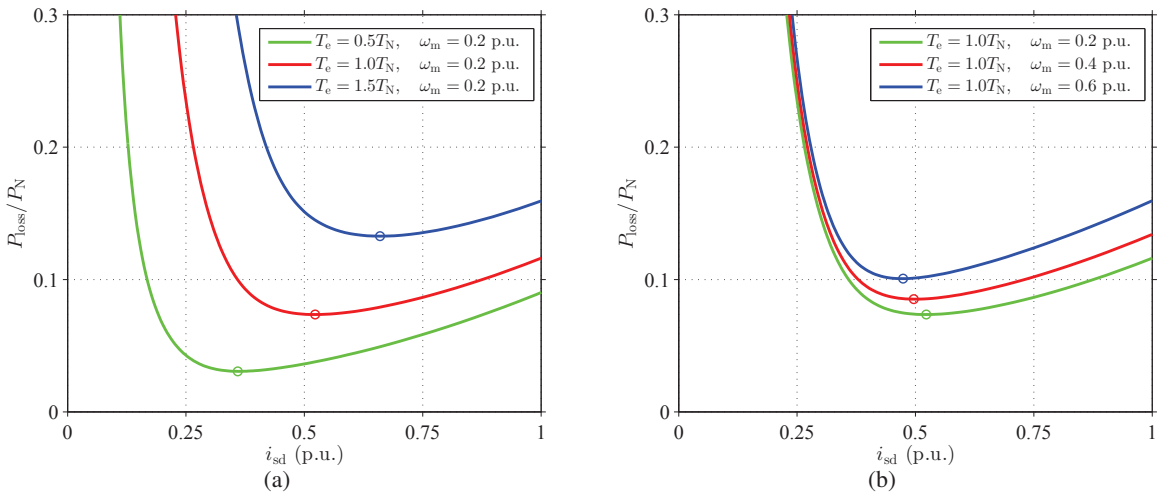

Figure 5: Calculated power losses of the 6.7-kW SyRM as a function of the d-axis current i_{sd}. The loss-minimizing points are marked by circles. (a) Loss curves are at the same speed $\omega_{\mathrm{m}} = 0.2$ p.u. and different torques $T_{\mathrm{e}} = 0.5T_{\mathrm{N}}, 1.0T_{\mathrm{N}}, 1.5T_{\mathrm{N}}$; (b) Loss curves are at rated load and different speeds $\omega_{\mathrm{m}} = 0.2$ p.u., 0.4 p.u., 0.6 p.u.

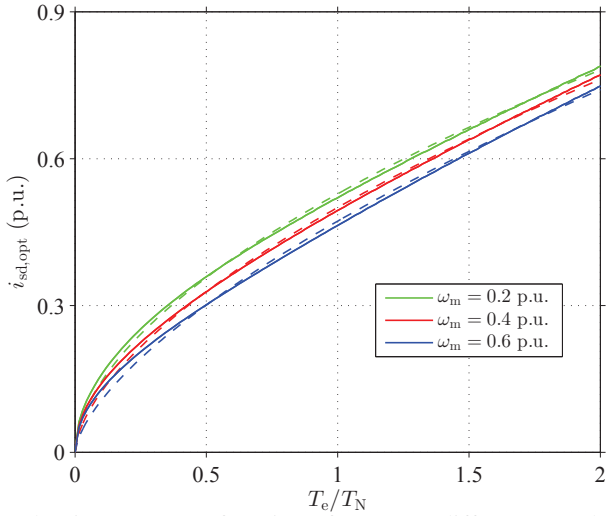

Figure 6: The loss-minimizing d-axis currents as function of torque at different speeds. The dashed lines are fitting results of the approximate function.

Comparison of the LMC with Conventional Methods

The loss-minimizing currents and the total losses using constant i_{sd}, the aforementioned conventional LMC and the proposed LMC are shown in Fig. 7. Results of 0.2 p.u. speed are shown as example. As can be seen, the proposed LMC saves significant losses compared to the method using a constant i_{sd} at low and high torque region. The discrepancy of the loss-minimizing currents of the conventional LMC and the proposed LMC is large. However, the difference of their losses is minor.

Experimental Validation

Experimental Setup

The analytical results of the loss-minimizing method are validated using experimental measurements. A transverse-laminated 6.7-kW four-pole SyRM is used in the laboratory. The rated values of the motor are: speed 3175 rpm; frequency 105.8 Hz; line-to-line rms voltage 370 V; rms current 15.5 A; and torque

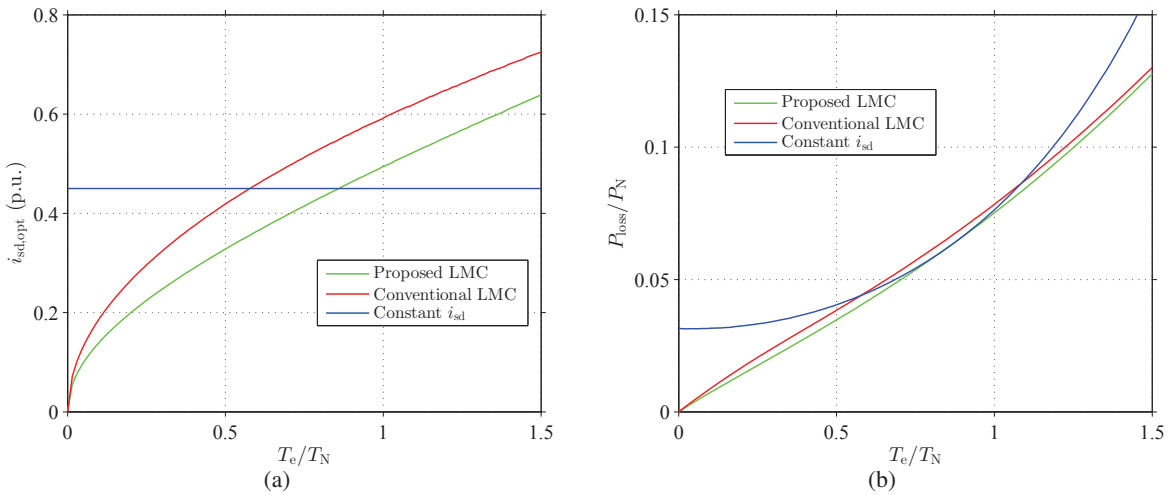

Figure 7: Comparison of the proposed LMC with the conventional LMC and constant i_sd. The speed is at 0.2 p.u. (a) The loss-minimizing d-axis currents as function of torque. (b) The calculated losses.

20.1 Nm. The SyRM is fed by a frequency converter controlled by a dSPACE DS1103 PPC/DSP board. A servo induction machine is used as a loading machine. The total moment of inertia of the experimental setup is 0.015 kgm^2. The load machine is controlled in torque-control mode and the studied SyRM is controlled in speed-control mode. The control system implemented in the DS1103 board is shown in Fig. 8. The loss-minimizing method is applied in a sensorless drive with a full-order flux observer [19].

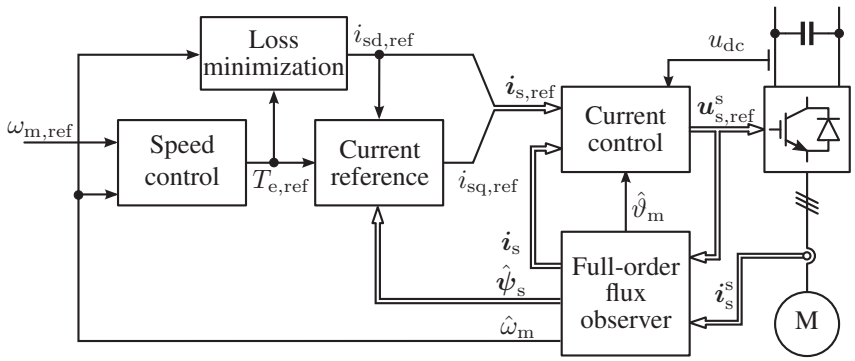

Figure 8: Loss-minimizing control of SyRM with full-order flux observer, where $\hat{\vartheta}_\mathrm{m}$ is the estimated electrical position, $\hat{\boldsymbol{\psi}}_\mathrm{s}$ the estimated flux, and $\hat{\omega}_\mathrm{m}$ the estimated speed.

Measurement Validation

In the experiments, the speed reference and load torque are kept constant while the reference i_sd is changed in small steps around the calculated optimal d-axis current value. The loss-minimizing current i_sd can be determined by the minimum input power. The stator currents are measured using LEM LA 55-P/SP1 transducers. The sampling is synchronized to the modulation, and both the switching frequency and the sampling frequency are 5 kHz (i.e., the sampling period $T_\mathrm{s} = 200$ μs). The reference voltage obtained from the current controller is used.

Fig. 9 shows one example of finding the loss-minimizing point for a given load and speed. The angular frequency is at 0.2 p.u. and the load reference is 80% of the rated torque. The d-axis current is changed in step of 2% of the calculated optimal value. The average input power is taken from steady state. As can be seen, the minimum input power is found at 5 s when the d-axis current is 0.432 p.u. By this approach, the loss-minimizing i_sd for different speeds and torques can be found. The experimental results are compared with the calculated loss-minimizing curves, which are shown in Fig. 10. It can be seen that the calculated results agree well with the experimental results.

It is worth noticing that in Fig. 9 the torque ripple and noise in the input power measurement are increased

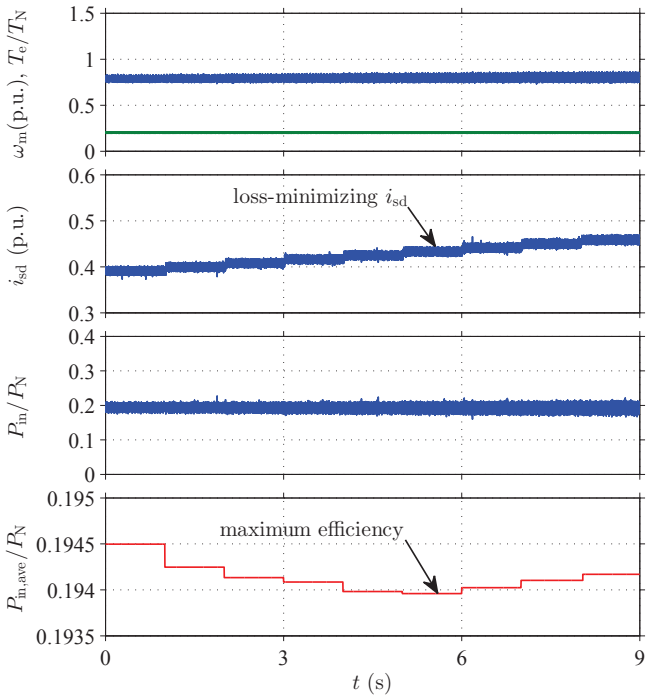

Figure 9: Experimental validation of loss-minimizing i_{sd} by input power measurement. The first subplot shows the load torque and the speed, the references of which are $0.8T_N$ and 0.2 p.u., respectively. The second subplot shows the d-axis current which is changed in steps around the calculated optimal value. The third subplot shows the measured input power. The last subplot shows the average input power in every step (transient period is excluded).

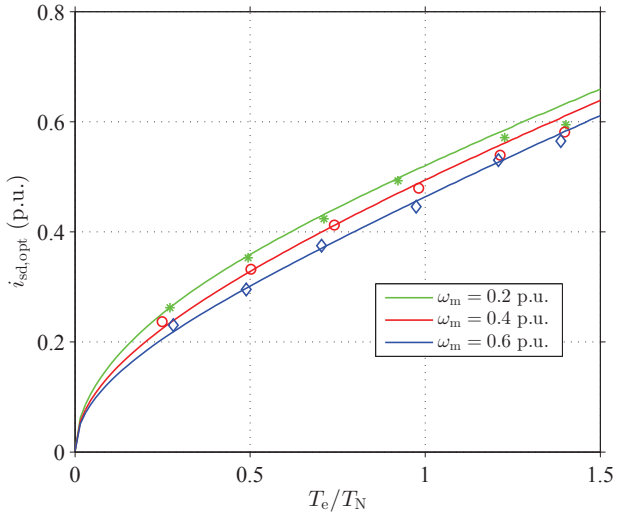

Figure 10: The calculated loss-minimizing i_{sd} curves (solid lines) and the loss-minimizing i_{sd} determined by experiments (markers)

with i_{sd}. As i_{sd} increases in the regenerating mode, the noise in the position estimate increases. This behavior suggests that the noise originates from saturation-induced harmonics. As the flux is increased, the unwanted spatial harmonics in the stator inductances are increased. These harmonics lead to slightly smaller optimal i_{sd} especially in the higher torque region. This explains the deviation of the calculated optimal current from the experimental results at higher load torque in Fig. 10.

Fig. 11 shows the experimental results of torque steps using the proposed LMC and constant i_{sd}. The speed is kept at 0.2 p.u. and the load torque is stepped from 0 to $0.64T_N$ at 2 s and $1.27T_N$ at 4 s. The minimum i_{sd} in the LMC is limited to 0.25 p.u. due to harmonics in the sensorless control at very low flux. The constant i_{sd} is 0.45 p.u. The corresponding values of the average input power are shown in Table II.

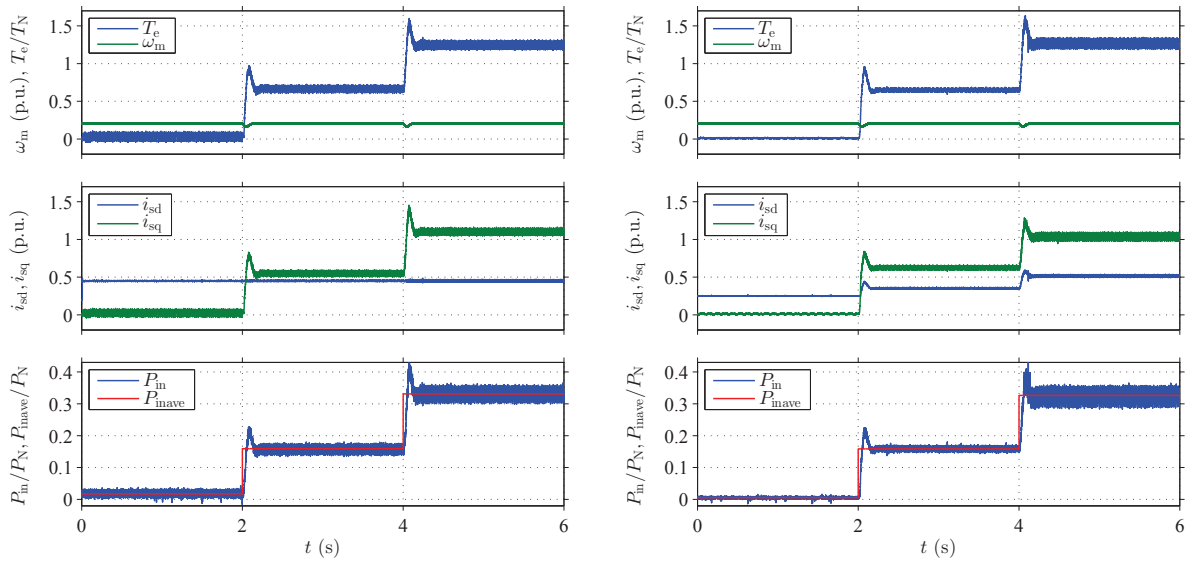

Figure 11: Load steps at constant speed. The first subplot shows the load and speed, the second shows the stator currents and the third shows the measured input power. (a) Constant i_{sd}. (b) proposed LMC.

Table II: The average input power of the proposed LMC and the method using constant i_{sd} in Fig. 11.

	Constant i_{sd}	LMC	Saved power
$T_{\mathrm{e}} = 0$	$0.017P_{\mathrm{N}}$	$0.005P_{\mathrm{N}}$	80.4 W
$T_{\mathrm{e}} = 0.64T_{\mathrm{N}}$	$0.1591P_{\mathrm{N}}$	$0.1587P_{\mathrm{N}}$	2.7 W
$T_{\mathrm{e}} = 1.27T_{\mathrm{N}}$	$0.331P_{\mathrm{N}}$	$0.326\ P_{\mathrm{N}}$	33.5 W

Conclusions

This paper proposed a maximum efficiency control for SyRMs taking both the core losses and magnetic saturation effects into account. The optimal currents are calculated offline using the motor parameters. The parameters of the core loss and magnetic saturation model are identified by experimental measurements. The calculated results are validated by measurements. Finally, the calculated results are fitted to an approximate function for online implementation. The loss-minimizing controller is applied in a sensorless drive system with a full-order observer. Since the optimisation process is performed offline, the online implementation is simple and requires low computation.

References

[1] S.-J. Kang and S.-K. Sul, "Efficiency optimized vector control of synchronous reluctance motor," in *Conf. Rec. IEEE-IAS Annu. Meeting*, vol. 1, San Diego, CA, Oct. 1996, pp. 117–121.

[2] J. H. Mun, J. S. Ko, J. S. Choi, M. G. Jang, and D. H. Chung, "Efficiency optimization control of SynRM drive using multi-AFLC," in *Proc. ICEMS'10*, Incheon, South Korea, Oct. 2010, pp. 908–913.

[3] J. E. Fletcher, B. W. Williams, and T. C. Green, "Loss reduction in a synchronous reluctance drive system using DSP control," in *Proc. IEEE PESC'95*, Atlanta, GA, Jun. 1995, pp. 402–407.

[4] T. Matsuo, A. El-Antably, and T. A. Lipo, "A new control strategy for optimum-efficiency operation of a synchronous reluctance motor," *IEEE Trans. Ind. Appl.*, vol. 33, no. 5, pp. 1146–1153, Sep./Oct. 1997.

[5] F. Fernandez-Bernal, A. Garcia-Cerrada, and R. Faure, "Efficient control of reluctance synchronous machines," in *Proc. IEEE IECON'98*, vol. 2, Aachen, Germany, Aug./Sep. 1998, pp. 923–928.

[6] H.-D. Lee, S.-J. Kang, and S.-K. Sul, "Efficiency-optimized direct torque control of synchronous reluctance motor using feedback linearization," *IEEE Trans. Ind. Electron.*, vol. 46, no. 1, pp. 192–198, Feb. 1999.

[7] W.-S. Baik, M.-H. Kim, N.-H. Kim, D.-H. Kim, K.-H. Choi, and D.-H. Hwang, "An optimal efficiency control of reluctance synchronous motor using neural network with direct torque control," in *Proc. IEEE IECON'03*, vol. 2, Roanoke, VA, Nov. 2003, pp. 1590–1595.

[8] T. Senjyu, K. Kinjo, N. Urasaki, and K. Uezato, "High efficiency control of synchronous reluctance motors using extended Kalman filter," *IEEE Trans. Ind. Electron.*, vol. 50, no. 4, pp. 726–732, Aug. 2003.

[9] I. Kioskeridis and C. Mademlis, "Energy efficiency optimisation in synchronous reluctance motor drives," *IEE Proc. Electr. Power Appl.*, vol. 150, no. 2, pp. 201–209, Mar. 2003.

[10] C. Mademlis, I. Kioskeridis, and N. Margaris, "Optimal efficiency control strategy for interior permanent-magnet synchronous motor drives," *IEEE Trans. Energy Convers.*, vol. 19, no. 4, pp. 715–723, Dec. 2004.

[11] J.-S. Choi, J. S. Ko, K.-T. Park, B.-S. Park, and D.-H. Chung, "Efficiency optimization control of SynRM drive by LM-FNN controller," in *Proc. ICPE'07*, Daegu, South Korea, Oct. 2007, pp. 373–377.

[12] C. Mademlis, "Compensation of magnetic saturation in maximum torque to current vector controlled synchronous reluctance motor drives," *IEEE Trans. Energy Convers.*, vol. 18, no. 3, pp. 379–385, Sep. 2003.

[13] S. Yamamoto, J. Adawey, and T. Ara, "Maximum efficiency drives of synchronous reluctance motors by a novel loss minimization controller considering cross-magnetic saturation," in *Proc. IEEE ECCE'09*, San Jose, CA, Sep. 2009, p. 288.

[14] T. Senjyu, T. Shingaki, and K. Uezato, "A novel high efficiency drive strategy for synchronous reluctance motors considering stator iron loss in transient conditions," in *Proc. IEEE PESC'01*, vol. 3, Vancouver, Canada, Jun. 2001, pp. 1689–1694.

[15] T. Senjyu, T. Shingaki, A. Omoda, and K. Uezato, "High efficiency drives for synchronous reluctance motors using neural network," in *Proc. IEEE IECON'00*, Nagoya, Japan, Oct. 2000, pp. 777–782.

[16] H. Aorith, J. Wang, and P. Lazari, "A new loss minimization algorithm for interior permanent magnet synchronous machine drives," in *Proc. IEEE IEMDC'13*, Chicago, USA, May 2013, pp. 526–533.

[17] Z. Qu, T. Tuovinen, and M. Hinkkanen, "Inclusion of magnetic saturation in dynamic models of synchronous reluctance motors," in *Proc. ICEM'12*, Marseille, France, Sept. 2012, pp. 992–998.

[18] D. W. Novotny, S. A. Nasar, B. Jeftenic, and D. Maly, "Frequency dependence of time harmonic losses in induction machines," in *Proc. ICEM'90*, vol. 1, Cambridge, MA, Aug. 1990, pp. 233–238.

[19] T. Tuovinen, M. Hinkkanen, L. Harnefors, and J. Luomi, "Comparison of a reduced-order observer and a full-order observer for sensorless synchronous motor drives," *IEEE Trans. Ind. Appl.*, vol. 48, no. 6, pp. 1959–1967, Nov 2012.